Sustainable Cities and Society 71 (2021) 102926

Contents lists available at ScienceDirect

Sustainable Cities and Society

journal homepage: www.elsevier.com/locate/scs

Surface urban heat island intensity in five major cities of Bangladesh: Patterns, drivers and trends

Ashraf Dewan [a,*], Grigory Kiselev [a], Dirk Botje [a], Golam Iftekhar Mahmud [b], Md. Hanif Bhuian [c], Quazi K. Hassan [d]

[a] School of Earth and Planetary Sciences, Curtin University, Kent Street, Bentley, Perth 6102, Western Australia
[b] Development Research Initiative, Dhaka, 1216, Bangladesh
[c] Department of Geography and Environment, Jagannath University, Dhaka, Bangladesh
[d] Department of Geomatics Engineering, University of Calgary, Calgary, Canada

ARTICLE INFO

Keywords:
Surface urban heat island
MODIS LST
Factors
Trends
Bangladesh cities

ABSTRACT

There is currently a lack of knowledge regarding the spatiotemporal variation of day and night surface urban heat island intensity (SUHII) in the major cities of Bangladesh. These cities have a large population base and generally lack the resources to deal with rapid urbanisation impacts, so any increase in urban temperature has the potential to affect people both directly (due to heatwave conditions) or indirectly (due to loss of livelihood). Time series diurnal (day/night) MODIS land surface temperature (LST) data for the period 2000–2019 was used to produce baseline information about SUHI intensity, drivers and temporal trends. Five large cities were selected based on population size and historical urban expansion rates. Results indicated that annual SUHII was greater in the larger cities of Dhaka and Chittagong than in the smaller cities. SUHII observed during the day was also greater than at night. Population (in terms of city size and surface cover), lack of greenness and anthropogenic forcing were major factors affecting SUHII. Trend assessments revealed positive trends during daytime in four out of five cities, while one city recorded negative trends at night. The findings may provide new insights into impacts arising from rapid urbanisation and demographic shifts.

1. Introduction

The world is currently experiencing widespread urban expansion, with the expansion rate equal to, or even higher than, the growth in the urban population (Seto, Fragkias, Güneralp, & Reilly, 2011). The world's total urban area has expanded by 168 % between 2001 and 2018, with the highest growth rates being observed in Asia and Africa (Huang, Huang, Wen, & Li, 2021). Cities and their inhabitants have become key drivers of global environmental change (Grimmond, 2007) due to a significant increase in human-created impervious areas around the globe (Gong et al., 2020). Urban expansion substantially alters natural surfaces, resulting in a range of environmental effects (Girardet, 2020). Though these effects can vary according to the scale of the study (Kalnay & Cai, 2003), they are most noticeable within local environments (Grimm et al., 2008).

The difference in temperature between the urban and surrounding rural areas is possibly the most visible effect associated with the urbanisation process and is mainly due to increased human activities (Heisler & Brazel, 2010). This observed temperature gradient is typically known as the urban heat island (UHI) – a phenomenon first noted in the European city of London in the early 1800's (Howard, 1833). The gradient is recorded as an index and flags the presence of elevated temperature locations within a city area. Two major types of UHIs are distinguished; a) the atmospheric urban heat island (AUHI), and b) the surface urban heat island (SUHI). The type of UHI is based on the height above the ground at which the phenomenon is observed and measured (Oke, 1982). UHIs modulate local climate (Landsberg, 1981; Roth, 2007), however they can also significantly influence both local and regional climates (Kalnay & Cai, 2003). There is a lack of consensus as to how UHIs contribute to global warming (Emmanuel & Krüger, 2012); the main disagreement being whether warming trend estimates derived from weather station data are influenced by local warming conditions (Zhou et al., 2004). Studies reveal, however, that the UHI contribution may be highly significant at the local scale, especially in rapidly growing

* Corresponding author at: Spatial Sciences Discipline, School of Earth and Planetary Sciences, Curtin University, Kent Street, Bentley, Perth, 6102 Western Australia.
E-mail address: a.dewan@curtin.edu.au (A. Dewan).

https://doi.org/10.1016/j.scs.2021.102926
Received 23 December 2020; Received in revised form 2 March 2021; Accepted 7 April 2021
Available online 15 April 2021

cities (Ren, Chu, Chen, & Ren, 2007). UHIs amplify thermal intensity (Estrada, Botzen, & Tol, 2017), so people residing in urban areas are becoming increasingly vulnerable to heatwave episodes (Liao et al., 2018). Mora et al. (2017) demonstrated that around 30 % of the world population is currently at risk of exposure to lethal heatwave conditions, a figure which is projected to increase to 48 % by 2100. Im, Pal, and Eltahir (2017) indicate that the densely populated agricultural region of South Asia may also experience extreme heatwave conditions in future. Apart from increasing heatwave likelihood, UHIs have the potential to impact human wellbeing and health (Pyrgou, Hadjinicolaou, & Santamouris, 2020), vegetation phenology (Kabano, Lindley, & Harris, 2021), diurnal temperature range (DTR) (Argüeso, Evans, Fita, & Bormann, 2014; Yang et al., 2020), energy consumption (Li et al., 2019), rate of disease vector development (Connolly, Keil, & Ali, 2020), water consumption (Guhathakurta & Gober, 2007) and can also lead to a general reduction in thermal comfort (Salata et al., 2017). With UHIs negatively impacting local environmental conditions (Parsaee, Joybari, Mirzaei, & Haghighat, 2019) and becoming a key challenge to achieving urban sustainability (Corburn, 2009), an increasing interest in assessing this phenomenon has taken place over the last decade or so (Giridharan & Emmanuel, 2018). Causal factors and the relative intensity of impacts vary according to latitude and/or climatic regions (Mirzaei & Haghighat, 2010), hence, many cities are now basing temperature adaptation/mitigation planning on local climatic conditions (Malings et al., 2017).

The techniques used to characterise UHI effect across cities can be broadly divided into: a) in-situ (field) measurements, and b) satellite-based estimation. In-situ observations, either by fixed weather stations or mobile traversing, are valuable in defining actual ground conditions (Hu, Xue, Klein, Illston, & Chen, 2016), however a change in location/instrumentation, as well as inadequate coverage, can complicate their use (Wang et al., 2007). To overcome these possible issues, land surface temperature (LST) data from airborne and earth observing satellites is commonly employed in UHI studies. In-situ air temperature records are typically used to examine AUHI, known as the canopy layer heat island (CUHI), and LST data is used to reveal the spatiotemporal pattern of SUHI. Remotely sensed data can provide synoptic and repeat coverage consistently over large areas, so they are widely utilised on: i) global (Chakraborty & Lee, 2019; Li, Zha, & Zhang, 2020; Peng et al., 2012; Schwarz, Lautenbach, & Seppelt, 2011); ii) regional (Fu & Weng, 2018; Imhoff, Zhang, Wolfe, & Bounoua, 2010; Raj, Paul, Chakraborty, & Kuttippurath, 2020; Tran, Uchihama, Ochi, & Yasuoka, 2006; Yao, Wang, Huang, Niu, Liu et al., 2018; Zhou, Zhao, Liu, Zhang, & Zhu, 2014); and iii) local scales (Hartz, Prashad, Hedquist, Golden, & Brazel, 2006; Lazzarini, Marpu, & Ghedira, 2013; Li et al., 2011; Mathew, Khandelwal, & Kaul, 2017; Tomlinson, Chapman, Thornes, & Baker, 2012; Wu, Ye, Shi, & Clarke, 2014). For example, Peng et al. (2012) used 419 global cities to demonstrate SUHI and associated causal factors. They showed that daytime surface urban heat island intensity (hereinafter, SUHII) is higher than nighttime, noting that the driving mechanisms differed according to the specific climatic zone within which the city was situated. Chakraborty and Lee (2019) emphasis that diurnal variability of SUHII is highest in equatorial climates and lowest in arid zones. Based on the data from more than 400 global cities, Li et al. (2020) note that factors influencing SUHII varied spatially between cities. Regional and city-specific studies such as those conducted in China, USA and India observe marked seasonality of SUHII (see Fu & Weng, 2018; Raj et al., 2020; Yao, Wang, Huang, Niu, Liu et al., 2018). For instance, satellite-based measurements of SUHII by Imhoff et al. (2010) indicate that the summer magnitude is larger than winter over 38 populous cities of the US. Likewise, Raj et al. (2020) note that SUHII is strongly influenced by rapid urbanisation in 44 Indian cities and nighttime trend is increasing. Huang et al. (2016) show that SUHII significantly influences the amplitude of daytime LST in Beijing and Shanghai, and that the DTR becomes narrower in Beijing and broader in Shanghai. Alexander (2021) reveals that causal factors of urban LST vary according to cities. Chen, Chiu, Su, Wu, and Cheng (2017) indicate that urbanisation strongly affects diurnal variation of cities temperature. Even though SUHII varies between cities, existing studies underscore the fact that human-dominated land use/cover changes, in combination with accelerated anthropogenic activities, are largely accountable for generating the excess heat recorded in urban agglomerations (Li et al., 2019; Lazzarini et al., 2013; Rodríguez, Ramos, de la Flor, & Domínguez, 2020), and therefore, location-specific measures are required to mitigate this (Li et al., 2020; Ren, Ng, & Katzschner, 2011).

Bangladesh, with an estimated total population of 161 million (m) and density of 1,120 per square kilometre (km^2) (BBS, 2012), is one country most vulnerable to climate change (Eckstein, Künzel, Schäfer, & Winges, 2019). The regional topography is characterised by a very low-lying land surface. It comprises eight administrative divisions, 64 districts and 12 city corporations. There are four distinct seasons: pre-monsoon (March–May), monsoon (June– September), post-monsoon (October–November) and winter (December–February). The climate is cool and dry during winter, with a hot humid summer and a rainy monsoon showing marked seasonality in both rainfall and temperature. Due to an ever–increasing population, the country has experienced, and continues to experience, a substantial reduction of existing natural surface (such as forest and agricultural lands), and an associated expansion in urban land (Rai, Zhang, Paudel, Li, & Khanal, 2017). The urban population of the country grew from 22.5 m in 1990 to 60 m in 2019 (https://data.worldbank.org/indicator/SP.URB.GROW? locations = BD; BBS, 2012), with resultant environmental issues in the major cities, including a sharp increase in observed temperatures (Kant, Azim, & Mitra, 2018). The trend of increasingly elevated temperatures in the main city is projected to increase, and continuous hot spell periods may become more common (Mourshed, 2011). Bangladesh is frequently affected by natural hazards such as flooding, so policies and strategies to minimise the impacts of these natural events are well developed. It is only recently, however, that urban warming has been recognised as an important issue affecting these large urban areas (GED, 2018).

Although the impact of land use/cover change on Landsat-based LST has been examined by many researchers (Gazi, Rahman, Uddin, & Rahman, 2020; Kant et al., 2018; Kafy, Rahman, Hasan, & Islam, 2020; Roy et al., 2020; Rahman et al., 2020; Trotter, Dewan, & Robinson, 2017), only two of them have examined SUHII (Kant et al., 2018; Roy et al., 2020). Another work utilises Moderate Resolution Imaging Spectroradiometer (MODIS) data of 2002–2014 during the monsoon season (June-August) over megacities of Asia, including Dhaka (Itzhak-Ben-Shalom, Alpert, Potchter, & Samuel, 2017). These works have improved the overall understanding of the spatiotemporal variation of LST/SUHII, however, they have used limited data (only daytime and selected years) and are limited in scope (e.g., using only a single city). The temporal resolution of Landsat is coarse (a 16-day cycle) and overpasses Bangladesh in the morning hours (10:30 am local time), so the use of Landsat data does not provide a complete picture of the real situation given that SUHI often intensifies later in the day (Guo et al., 2015). Landsat also does not provide nighttime data, which hinders estimation of the intensity of SUHI during the night. Existing studies have also only examined the relationship between vegetation and LST, but it is highly likely that SUHII is also influenced by multiple other factors (Li et al., 2020). Kotharkar, Ramesh, and Bagade (2018), in a critical review of existing research, demonstrate that baseline data about UHIs of Bangladesh cities is clearly lacking. The review notes that Delhi, Chennai and Colombo were the most frequently studied cities in South Asia. It is important to note that the intensity and magnitude of day and nighttime SUHI varies between cities, even if they are in the same country (Huang et al., 2016).

Many studies utilise infrared-derived LST data from satellites, such as MODIS, however a shortcoming with these measurements is that valid data is restricted to clear-sky conditions (without cloud). Chakraborty, Hsu, Manya, and Sheriff (2020) note that, as the recorded LST values are valid only for clear-sky conditions they may not represent the

climatological mean state. Ermida, Trigo, DaCamara, Jiménez, and Prigent (2019) use passive microwave LST observations to overcome the infrared-based limitations and note that the amplitude of clear-sky bias (the difference between average clear-sky and average all-weather LSTs) is closely related to the fraction of clear-sky days. These observations are pertinent in countries where seasonal cloud cover can be an issue.

Existing studies may be of little relevance for the expanding cities of Bangladesh (from the viewpoint of mitigating the negative impacts) for a number of reasons. Firstly, global studies are based on a stationary urban boundary, hence are prone to uncertainty (Manoli et al., 2019). Findings are therefore difficult to implement on a local level (Chakraborty et al., 2020). Secondly, satellite observation time greatly influences SUHI intensity owing to the fact that the overpass time differs between cities (Mathew, Khandelwal, Kaul, & Chauhan, 2018). Thirdly, energy and health impacts vary between day and night, so characterising the full diurnal scale of local climate is essential (Krayenhoff, Moustaoui, Broadbent, Gupta, & Georgescu, 2018). Fourthly, measures undertaken to curb urban warming during summer may intensify SUHI intensity in winter (Debbage & Shepherd, 2015). Finally, previous studies have not comprehensively examined the spatiotemporal patterns of urban warming, its determinants and trends over these cities, although these types of studies are crucial for a populous and data poor country like Bangladesh. The identification of city–scale warming patterns can contribute to informed decision–making and support the new "smart city" concept aimed at promoting sustainable urban development. The findings can also be of value in developing location–specific adaptation strategies to reduce environmental impacts related to urbanisation–induced local warming and to improve the quality of life of the urban dwellers.

The primary aim of this study is to develop baseline information on the spatiotemporal pattern of SUHII in selected cities of Bangladesh using timeseries MODIS LST data. Five large cities, namely Dhaka, Chittagong, Khulna, Rajshahi and Sylhet, have been selected based on population size, historical urban growth (BBS, 2012; Rai et al., 2017) and the availability of ancillary information. The objectives are to: (a) examine annual and monthly day, night SUHII between 2000 and 2019; (b) determine factors controlling SUHII in these cities; and (c) investigate temporal trends.

2. Materials and methods

2.1. Datasets

The MOD11A2 LST product (v006) used in this study is 1 km spatial resolution, 8-day composite data averaged from MODIS daily observations (10.30 am and 10.30 pm) for the 2000–2019 period. Version 6 data is used in this study due to its improved accuracy (Wan, 2014). The LST has been retrieved from MODIS 31 and 32 bands using a generalised split-window algorithm. The initial LST retrieval has been corrected for cloud contamination issues, so this study uses imagery with only clear sky pixels and has been subsequently processed to retain pixels with an LST error of $\leq$2 K.

Other Version 6 MODIS products used include yearly land use and land cover (LULC) (MCD12Q1), an 8-day surface reflectance product (MOD09A1), a daily aerosol optical depth (AOD) product at 0.55 μm (MCD19A2), a daily short-wave black and white sky albedo (MCD43A3) product and vegetation continuous function product (MOD44B). Gridded population data includes annual LandScan data at 1 km spatial resolution (https://landscan.ornl.gov/), which provides people per pixel and an average of the 24 -h population. To understand the contribution of anthropogenic forcing, nighttime lights (NTL) data was used, comprising both the Defence Meteorological Satellite Program – Operational Linescan system (DMSP-OLS) and the Visible Infrared Imaging Radiometer Suite (VIIRS) data. The NTL data has undergone intercalibration, intra-annual composition, inter-annual corrections (Liu, He, Zhang, Huang, & Yang, 2012) and cross-sensor calibration. A power function, similar to that documented in Wu, He, Peng, Li, and Zhong (2013), was used to intercalibrate the DMSP-OLS data. This function was specifically used to obtain the regression coefficients representing the relationship between invariant regions of one reference and the other DMSP-OLS images. These coefficients were subsequently used to develop the intercalibrated DMSP-OLS data. The F152001 image was used as a reference image in this case. Invariant regions were then defined from groups of pixels, with each pixel having a standard deviation of $\leq$1.5 for the whole 2000–2013 timeseries. To integrate the VIIRS data with DMSP-OLS, the seasonality of VIIRS was initially removed using the Hodrick and Prescott (1997) filter and then the Biphasic Dose Response (Ma, Guo, Ahmad, Li, & Hong, 2020) model was used to cross-calibrate both NTL annual series. A nominal resolution of 1 km was used to make all the datasets consistent.

This study utilises the planning boundary of the five cities rather than the city corporation area for analysis, since all future urban growth will definitely take place within this defined planning zone. A shape file of each planning boundary was acquired from the relevant city development authorities.

2.2. Analytical techniques

Yearly MODIS LULC data, using the International Geosphere-Biosphere programme (IGBP) classification scheme (Sulla-Menashe & Friedl, 2018), was employed for this study. Several steps were involved in defining urban and rural areas using the LULC data. Firstly, the data was reclassified into urban and non-urban land covers. This was an iterative process to define multitemporal urban boundary (2000–2019) for each city. Secondly, a buffer polygon, away from the urban area was created to define the rural boundary. Twenty buffer polygons were generated for each year (2000–2019) given the number of urban pixels change every year, and to ensure that the size of the rural area being approximately the same as urban area for each city. Due to dissimilarities in the size of the cities, some adjustments to buffer size were required. For example, the rural buffer for Dhaka was 20 km away from existing urban cover (Fig. 1) while for Rajshahi it was 15 km. The rational regarding the buffer distance variability was that a greater distance from the defined urban pixels would provide an increased accuracy in SUHI values (Zhou et al., 2014). Waterbodies in urban areas, as well as built-up pixels in rural sites, can potentially influence the accuracy of SUHI intensity calculations (Chakraborty & Lee, 2019; Li et al., 2020), so these were removed. Finally, the LST values for urban and rural areas were extracted for each month/year (day and night), for each city. The intensity of SUHI (SUHII), i.e., the difference in mean LST between urban and rural areas, was then defined for each city. To examine the spatial pattern of SUHII, the pixel-wise difference in mean LST was used.

A number of indices were computed from the highest quality pixels of MODIS timeseries 8-day reflectance product. They were: enhanced vegetation index (EVI) (Liu & Huete, 1995), otherwise known as greenness; normalised difference water index (NDWI) (McFeeters, 1996); biophysical composition index (BCI) (Deng & Wu, 2012); and moisture stress index (MSI) (Rock, Vogelmann, Williams, Vogelmann, & Hoshizaki, 1986). The reason for using EVI instead of the most popular normalised difference vegetation index (NDVI) is that NDVI is prone to saturation (Li et al., 2011). BCI was chosen due to its effectiveness in separating impervious surfaces from other urban land cover categories (Deng & Wu, 2012). The coefficients utilised in calculating the tasselled cap transformation were obtained from Wu, Xiong et al. (2013), and were then used to compute BCI. Since waterbodies have specific heat capacity and influence both heating and cooling of urban environment (Tan, Sun, Huang, Yuan, & Hou, 2021), NDWI was used. The availability of soil and plant moisture can also significantly modulate urban thermal environment. To understand the effect of moisture on SUHI intensity, MSI was employed. Equations used to derive these indices are shown in supplementary Table S1. Derived indices were then aggregated at

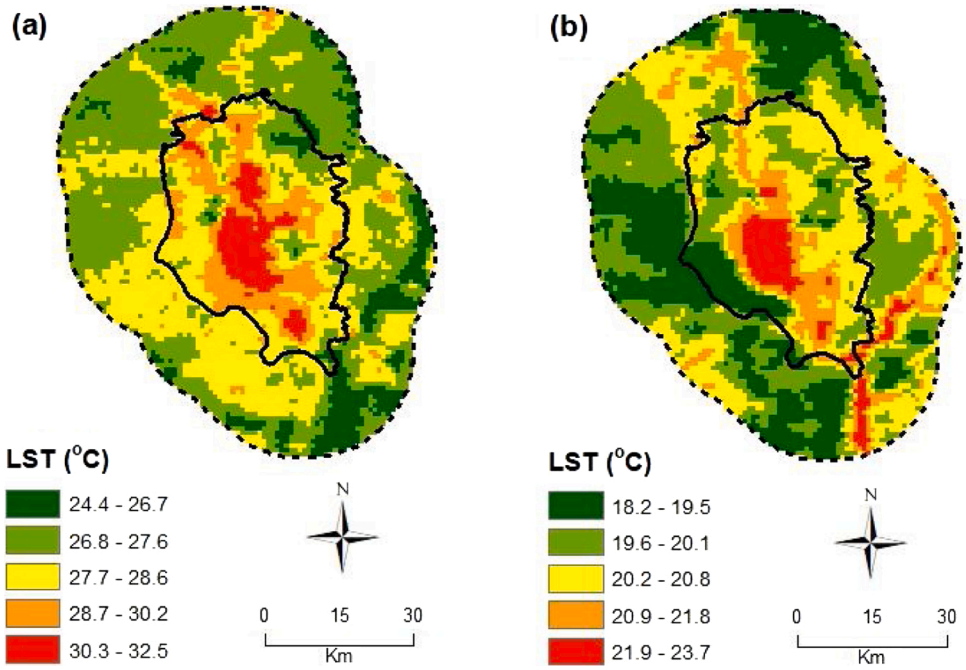

Fig. 1. Average land surface temperature (LST) of 2019 in Dhaka megacity and delineation of urban and rural boundaries; (a) day; (b) night. Black solid polygon is Dhaka Metropolitan Development Plan (DMDP) boundary and dashed line is the buffer polygon location.

monthly and annual scales. Other potential causative factors identified included AOD, population, NTL, VCF and albedo. Since black-sky and white-sky albedo are linearly related and provide similar result (Peng et al., 2012), only white-sky albedo (WSA) was used. The tree cover fraction of annual VCF product (Dimiceli et al., 2015) was also utilised.

A number of steps were performed to isolate potential factors affecting SUHI intensity. Initially, the delta values of each causative variable between urban and rural areas (δAOD, δBCI, δEVI, δPOP, δMSI, δNDWI, δNTL, δTREE and δWSA) were extracted. Scatterplots were produced from the temporally-averaged day and night SUHII of all cities (calculated from the annualised mean) and the explanatory variables, and were used to explore the variable relationships (supplementary Fig. S2). Prior to conducting the correlations, the multicollinearity between independent variables was also tested using the variance inflation factor (VIF). In this process, all the variables were used to identify the suitability of individual variables and variable combinations. Factors exhibiting high VIF were removed, predictors that were linearly uncorrelated were isolated and parameters having a VIP value of <10 (Lin, 2008) were retained. To determine the temporal relationship between each environmental factor and SUHII, twenty samples (2000–2019) for each city was used. The Pearson's correlation coefficient (r) and tests for significance at 95 % and 99 % levels were performed.

The temporal trends of annualised day and nighttime means of SUHII over five cities were evaluated using the Mann-Kendall (MK) test (Kendall, 1948; Mann, 1945). The slope of the trend was estimated using the Theil-Sen slope (Sen, 1968), with a positive value of the slope indicating an increasing trend and a negative value denoting a decreasing trend. The corresponding *p*-value was also estimated (at 95 % and 99 % significance levels), to indicate whether the observed SUHII trend is statistically significant or not.

Finally, to determine the relative impact of cloud cover on clear-sky pixel retrieval, pixel loss due to cloud was also calculated. The data was first decoded and then the mandatory QA (MODLAND) scientific dataset was clipped using the buffers and cloud cover pixels (value 10) were removed from the total pixel count for each image to provide a pixels lost/pixels retained percentage.

3. Results

3.1. Variability of day and nighttime SUHII

The average SUHII of the cities is shown in Fig. 2. This indicates that the annual daytime SUHII is greatest for Dhaka (2.74 °C), followed by Chittagong (1.92 °C), Khulna (1.27 °C), Sylhet (1.10 °C) and Rajshahi (0.74 °C). In contrast, nighttime mean SUHII is greatest for Chittagong (1.90 °C), with Dhaka second (1.57 °C). The lowest nighttime SUHII is observed in Sylhet city (0.16 °C). The annual average SUHII for day and nighttime is positive for all five cities, though the magnitude differs. This may be related to the city area and population size of these cities.

The spatial pattern of annual day and night SUHII is presented in Fig. 3. This indicates that SUHII is mainly concentrated in the urban core, both during the day and at night. For instance, the main urban core of Dhaka experiences values as high as 5 °C while SUHII values for Chittagong ranges from 2 to 3 °C during the daytime. At night, elevated temperatures are recorded in the urban core of both cities.

Inter-annual day, night and day-night SUHII variability are shown in Fig. 4. The Dhaka daytime SUHII exhibits a notable increase in mean temperature from 2.20 °C in 2000 to 3.18 °C in 2019. The equivalent time period values for Chittagong are 1.80 °C and 2.28 °C, indicating an increase of 0.48 °C during that 20-year period. In contrast, the difference in SUHII during the day for Khulna, Rajshahi and Sylhet is 0.57, 0.04 and 0.38 °C, respectively, for that period. This suggests that Dhaka has experienced the greatest increase in daytime SUHII (0.98 °C) whereas Rajshahi has the least (0.04 °C). In regards the nighttime SUHII, Chittagong has the largest increase (0.52 °C) followed by Sylhet (0.34 °C), Rajshahi (0.25 °C) and Dhaka (0.23 °C). Surprisingly, Khulna has experienced a drop of 0.34 °C in nighttime SUHII since 2000. The day-night variability is high for Chittagong followed by Rajshahi, while Dhaka, Sylhet and Khulna appear to show a subtle variation. This may point to narrowing/broadening of the DTR over time (Fig. 4). The monthly variation of day and night SUHII, and diurnal range, is shown in supplementary Fig. S3.

Monthly day and night SUHII for the five cities were averaged and are shown in Fig. 5. This shows that month-wise day and nighttime SUHII varies substantially between the cities. In Dhaka, for example,

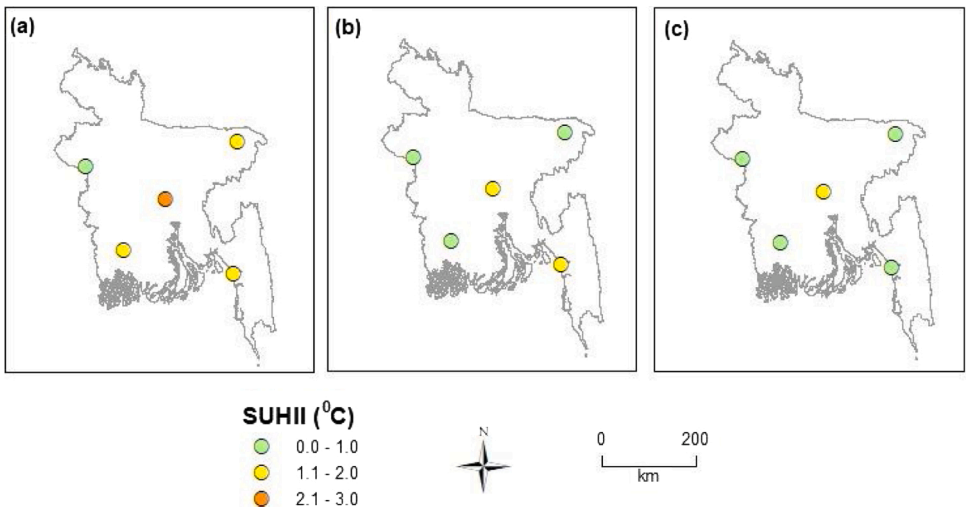

Fig. 2. (a) Daytime; (b) nighttime surface urban heat island intensity (SUHII); and (c) diurnal range over five Bangladesh cities, averaged over 2000–2019.

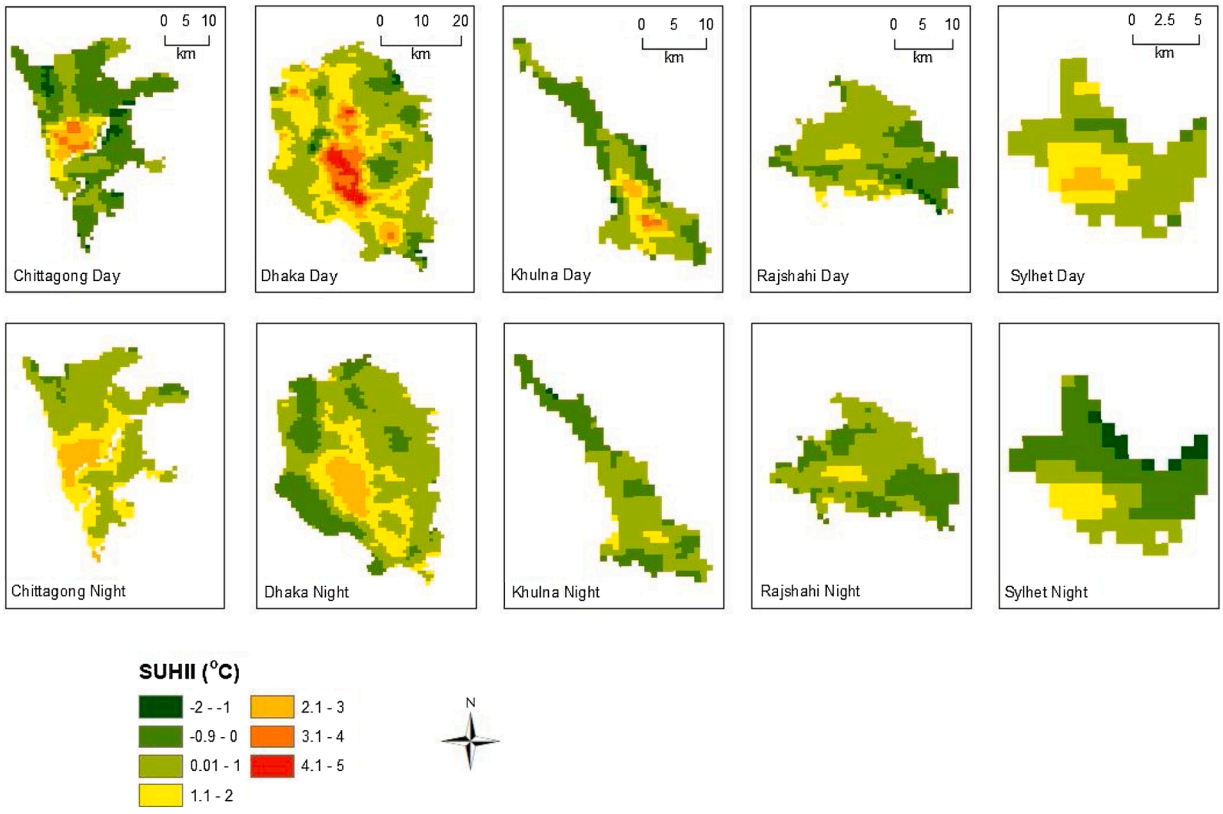

Fig. 3. Spatial pattern of surface urban heat island intensity (SUHII) in five cities, averaged over 2000–2019; (a) day; (b) night.

high SUHII values occur in August (3.52 °C) during the day, and in January (2.16 °C) at night. In Chittagong, the daytime maximum SUHII takes place in September (3.14 °C) while the nighttime maximum occurs in January (2.40 °C). Khulna experiences mostly positive daytime SUHII (except during the months of June and July). At night, the months of July to October exhibit negative SUHII. The highest SUHII is seen in September (1.52 °C) during the day and in March (1.06 °C) during the night. Positive SUHII dominates during both day and night, with the exception being the negative SUHII observed in Rajshahi during August nighttime and December daytime. Interestingly, both maximum day (3.10 °C) and night (1.99 °C) SUHII occur during the month of July in this city, located in northern Bangladesh. The intensity of SUHII appears to vary significantly in Sylhet city since negative SUHII dominates during the night as compared to daytime. June records negative day and night SUHII, with May having the highest SUHII (1.74 °C) during the day and during nighttime, and February having the highest SUHII (1.06 °C). The intensity of daytime SUHI is generally the same, while the nighttime intensity varies according to city size, indicating that the day-night

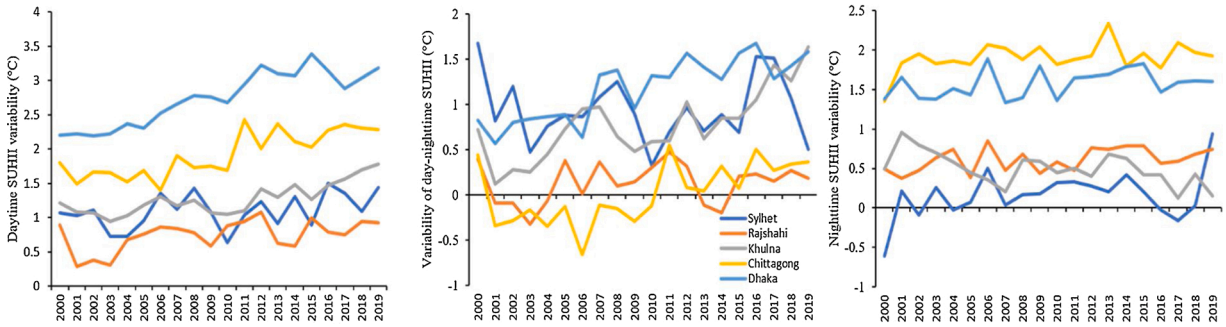

Fig. 4. Day, night and day-night inter-annual variability of surface urban heat island intensity (SUHII) in five cities, 2000–2019.

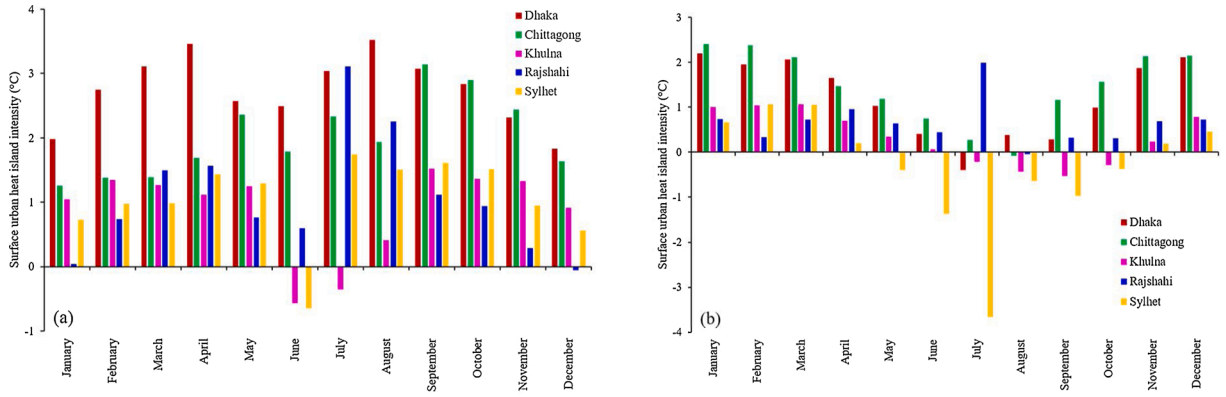

Fig. 5. Monthly surface urban heat island intensity (SUHII) in five cities averaged over 2000–2019; (a) Day; (b) Night.

variability of urban temperature is decreasing in the larger cities such as Chittagong.

3.2. Factors associated with SUHII

The VIF values of the original nine explanatory variables are shown in supplementary Table S4. The analysis reveals that three variables (e.g., EVI, MSI and NDWI) have high VIF values across all cities. On the other hand, BCI shows a linear relationship with variables such as NTL. Following further analysis, the results indicate that four cities (Dhaka, Chittagong, Khulna and Rajshahi) can be explained by a common set of variables while Sylhet cannot (Table 1). A high VIF value is observed between δPOP and δNTL for Sylhet, while removing NTL provides acceptable VIF values (Table 1). It would be expected that EVI (live vegetation or its growth status) and VCF (tree cover per pixel) should have a strong association, however this does not appear to be the case. Seven variables were identified as free from collinearity issues and were used to evaluate the relationship between SUHII and any potential drivers.

Table 1
Variance inflation factor (VIF) for explanatory variables.

Variable	Variance Inflation Factor (VIF)				
	Dhaka	Chittagong	Khulna	Rajshahi	Sylhet
δAOD	2.177	2.023	1.439	1.321	1.403
δBCI	–	–	–	–	2.464
δEVI	6.640	5.019	1.790	6.106	3.740
δPOP	3.570	2.991	1.700	3.432	2.215
δNTL	2.241	5.541	2.511	6.526	–
δVCF	1.413	1.204	1.460	1.262	1.349
δWSA	1.275	2.623	1.743	1.262	3.279

Table 2 displays the correlation between SUHII and a number of possible driving factors. Results indicate that greenness, as defined by the difference in EVI between the urban and rural areas, has a consistently negative relationship with day and nighttime SUHII. This suggests that vegetation plays a key role in regulating the surface temperature of these cities (with the exception of nighttime in Khulna). A statistically significant relationship between daytime SUHII and the urban and rural population difference (δPOP) is observed in three cities, and at night in Rajshahi.

BCI appears to be linearly related to other variables in four cities, and it shows a significant influence on nighttime temperature in Sylhet. This is evidence for the influence of impervious surfaces on temperature. Anthropogenic forcing, defined by δNTL, is negatively correlated for Dhaka, but shows statistically significant positive relationships for Chittagong (both during day and night) and during the day for Khulna and Rajshahi.

The relationship between albedo (δWSA) and SUHII appears to be rather inconsistent. For instance, WSA has a significantly positive relationship with daytime SUHII in Chittagong and Khulna. However, such a relationship is negative and mostly weak for the other cities (both day and night). The effect of aerosol on temperature is negative during the day and nighttime for Dhaka and Chittagong, however other cities show a weaker and statistically insignificant relationship. Tree cover, obtained from δVCF, has a weakly positive correlation during day across cities, but at night, the relationship is negative for Dhaka and Khulna with a much lower correlation coefficient (Table 2). The correlations between monthly SUHII and the difference in causative factors also show similar results (data not shown).

Table 2
Pearson's correlations between annual day and night surface urban heat island intensity (SUHII) and factors across cities.

Factors	Dhaka		Chittagong		Khulna		Rajshahi		Sylhet	
	Day	Night	Day	Night	Day	Night	Day	Night	Day	Night
δAOD	−0.372	−0.213	−0.325	−0.429	−0.142	0.117	0.322	−0.015	0.089	0.031
δBCI	–	–	–	–	–	–	–	–	0.381	0.467**
δEVI	−0.891*	−0.491**	−0.863*	−0.318	−0.766*	0.456**	−0.371	−0.508**	−0.391	−0.567*
δPOP	0.919*	0.458	0.718*	−0.135	0.385	−0.342	0.496**	0.600*	0.370	0.389
δNTL	−0.364	−0.140	0.770*	0.451**	0.603*	−0.625*	0.534**	0.407	–	–
δVCF	0.310	−0.070	0.061	0.099	0.066	−0.180	0.226	0.154	0.266	0.243
δWSA	−0.149	−0.286	0.515**	0.154	0.626*	−0.795*	−0.299	−0.226	−0.115	−0.388

* Significant at 99 %.
** Significant at 95 %.

3.3. Trends of SUHII

Annual day and nighttime SUHII trends (obtained via Mann-Kendall test) are shown in Table 3. This indicates that the daytime SUHII trend appears to be increasing for four of the five cities, with Chittagong, Khulna and Rajshahi exhibiting a statistically significant trend. During nighttime, however, only Rajshahi has a statistically significant increasing trend, and Dhaka, Chittagong and Sylhet show an insignificantly positive trend. In contrast, Khulna city exhibits a decreasing trend in regards nighttime SUHII.

Monthly SUHII trends are presented in Table 4. Dhaka shows an increasing trend during day across all months except July, while at night the months of May, July and August show negative trends, though the magnitude of the trends differs. Chittagong has an overall positive daytime trend (apart from August), but the trend decreases during nighttime in May and August. Khulna shows a nighttime negative trend for nearly all months (again with the exception of August). Daytime SUHII however shows an overall positive trend (apart from July). Rajshahi experiences an increasing daytime trend for most months, while at night only April shows a decreasing trend. Sylhet, in contrast, exhibits a daytime increase, except in June and August. During the night only May shows a negative trend.

Table 3
Annual day and nighttime trend of SUHII in five cities (°C/y).

Time	Dhaka	Chittagong	Khulna	Rajshahi	Sylhet
Daytime	0.062	0.046*	0.032*	0.020**	0.017
Nighttime	0.012	0.007	−0.021	0.012**	0.015

* Significant at 99 %.
** Significant at 95 %.

3.4. Clear-sky pixel count

The percentage of LST pixels remaining after removal of defined cloud-affected data, but before further processing, is shown in Table 5.

Table 4
Monthly day and night trend of SUHII for five cities (°C/y).

Mon	Dhaka		Chittagong		Khulna		Rajshahi		Sylhet	
	Day	Night	Day	Night	Day	Night	Day	Night	Day	Night
Jan	0.060*	0.023**	0.033*	0.010	0.020	−0.026*	0.048*	0.006	0.013	0.008
Feb	0.067	0.037*	0.029	0.015	0.026	−0.003	0.014	0.003	0.003	0.011
Mar	0.063*	0.029	0.042	0.024	0.025	0.002	0.016	0.011	0.050	0.038*
Apr	0.090*	0.012	0.092*	0.016	0.035	−0.017	0.048**	−0.003	0.051**	0.045
May	0.025	−0.015	0.037	−0.018	0.032	−0.025	0.032	−0.046*	0.082**	−0.005
Jun	0.093	0.032	0.119	0.044	0.056	−0.001	0.081**	0.068**	−0.153	0.144**
Jul	−0.022	−0.018	0.099	0.051	−0.098	−0.034	0.001	0.012	0.072	0.000
Aug	0.006	−0.010	−0.012	−0.091	0.129*	0.024	0.006	0.008	−0.066	0.001
Sept	0.071**	0.010	0.099*	0.011	0.064*	−0.025	0.044	0.016	0.015	0.042**
Oct	0.059*	0.010	0.069*	0.036**	0.061*	−0.008	0.037	0.030**	0.014	0.019
Nov	0.049*	0.028*	0.061	0.019	0.024	−0.038*	−0.014	0.029*	0.016	0.015
Dec	0.039*	0.010	0.025	0.013	0.024**	−0.046	−0.008	0.012*	0.004	0.005

* Significant at 99 %.
** Significant at 95 %.

Table 5
Percentage of pixels (%) remaining after removal of cloud–affected pixels.

Period	Dhaka		Chittagong		Khulna		Rajshahi		Sylhet	
	Rural	Urban	Rural	Urban	Rural	Urban	Day	Night	Day	Night
Annual day	75.9	72.9	73.9	74.8	75.9	73.9	75.6	75.7	73.8	71.6
Annual night	74.1	73.9	69.6	70.5	75.0	74.8	77.2	77.6	72.1	71.9
Pre-monsoon day	91.2	90.5	87.5	89.0	93.0	91.6	94.2	94.8	85.4	84.1
Pre-monsoon night	94.4	93.5	95.4	95.3	94.5	94.4	96.7	97.1	85.4	85.7
Monsoon day	37.4	28.6	34.4	35.7	36.3	30.0	34.8	33.8	34.9	29.1
Monsoon night	28.9	29.3	15.4	18.1	31.0	30.4	35.4	36.5	28.9	28.0
Post-monsoon night	98.2	98.0	96.5	97.4	98.8	99.1	97.8	98.2	98.5	98.5
Post-monsoon night	97.1	96.5	95.7	95.6	98.1	97.9	99.0	99.0	98.7	98.6
Winter day	96.8	97.7	97.8	97.8	96.4	98.0	96.6	97.6	97.6	97.9
Winter night	98.6	98.7	98.7	98.8	98.7	98.7	98.7	98.7	98.7	98.7

Further statistics for each aggregated period are contained in supplementary Table S5 which illustrates the impact of cloud cover on the base diurnal LST value counts, annually and seasonally, for the five cities. There is minimal loss of pixels in the post-monsoon and winter periods, with > 95.6 % valid pixels recorded over the city areas during both day and night. The counts during the pre-monsoon season indicate that most urban and rural areas recorded average valid pixel counts of approximately 90 %, although Sylhet, located in a topographically elevated region in the north-east of the country recorded 85 % valid pixels during both day and night. The monsoon period, characterised by heavy rainfall and extensive cloud cover, shows average valid pixel counts for all cities of 35.6 % for rural day time, 31.4 % for urban daytime, 27.9 % for rural nights and 28.5 % for urban nights. Chittagong, the only city located next to the ocean, recorded 34.4 %–35.7 % for daytime (on par with other cities) but a very low 15–18.1 % for monsoon nights. This may be the result of oceanic influences during nighttime. Using the term clear-sky pixel as an indication of individual LST robustness is appropriate, however the term is questionable if used during monsoonal periods when a significant reduction in valid pixels may impact areal LST calculations.

4. Discussion

A rapid growth in population and the associated urban areas are recognised as significant and active agents of local temperature change (Chapman, Watson, Salazar, Thatcher, & McAlpine, 2017), especially in developing countries. Urbanisation, in combination with global warming, is expected to increase heat-related mortality (Mora et al., 2017). Cities in developing countries typically have large populations and generally lack the resources to deal with the consequences of rapid urbanisation (Moretti, 2014), so a consistent rise in temperature in these areas has the potential to negatively impact the lives and livelihood of millions (Huq, 2001). Evaluating the spatiotemporal pattern of urban warming, as well as identifying possible causal factors, is the first step in the development of possible adaptation measures (Ren et al., 2011). This process appears to be currently lacking for the cities of Bangladesh.

No comparable studies are available to validate the SUHII variation observed in the current analysis, however the Chakraborty and Lee (2019) study has provided an opportunity to compare results. For example, this work found that the annual day and nighttime SUHII values were 2.74 and 1.57 °C for Dhaka, while their study reported 1.60 and 1.03 °C, respectively. Likewise, SUHII values for other cities tended to vary between the two studies though the spatial patterning was very similar. The strongest SUHII was mainly confined to the urban core during both day and night (Fig. 3), which may be related to high population density as well as other sociocultural factors such as income and access to transportation (Chakraborty et al., 2020). Surface roughness of the urban areas (Hu et al., 2016) could also be important. A comparison of monthly SUHII values across the cities revealed some similarities in the observed variation. Observed discrepancies in day/night SUHII values may have resulted from the data and methods used (Yao, Wang, Huang, Niu, Chen et al., 2018). For instance, Chakraborty and Lee (2019) used both Aqua (MYD) and Terra (MOD) LST datasets from 2003 to 2018 with a calculated LST error of ≤3 K. MYD data is collected during overpasses at 1.30 pm and 1.30 am in contrast to the 10.30 am and 10.30 pm collection time for MOD. The current study utilised 20 years (2000–2019) of data from only the Terra sensor, with a defined LST error of ≤2 K. Previous studies have shown that variations in the MODIS quality flag use can significantly impact the estimation of SUHII (Lai et al., 2018). The number of samples obtained can have a significant effect (de Faria Peres, de Lucena, Rotunno Filho, & de Almeida França, 2018), and the environmental condition of the overpass area also affects SUHII characterisation (Kerr, Lagouarde, Nerry, & Ottlé, 2004). Differences in the delineation of the defined urban extent is another possible area of variation. As noted earlier, city-specific SUHII studies of Bangladesh are virtually non-existent, however previous studies with selected Landsat data (Kant et al., 2018; Roy et al., 2020) had indicated an increased daytime SUHII, corroborating the current findings. The impact of land use change on LST produced a similar outcome for Rajshahi (Kafy et al., 2020) and Dhaka (Rahman et al., 2020; Trotter et al., 2017). It is, therefore, reasonable to say that this work has provided important baseline information on monthly and annual intensity of SUHI, during the day and night, and that larger cities appear to have greater variation than smaller cities. This contrasts with the findings of Peng et al. (2012).

The temporal evolution of SUHII indicated that the warming trend was intensifying over time, particularly in Dhaka and Chittagong (Fig. 4). Studies undertaken on global to local scales have also observed this phenomenon; a response to increased anthropogenic forcing and heterogeneous urban mosaics irrespective of climatic zone (Alexander, 2021; Bowler, Buyung-Ali, Knight, & Pullin, 2010; Coseo & Larsen, 2014; Deilami, Kamruzzaman, & Liu, 2018; Hu et al., 2016; Lai et al., 2018; Li et al., 2020; Peng et al., 2019; Quan, Zhan, Chen, Wang, & Wang, 2016; Raj et al., 2020; Yao, Wang, Huang, Niu, Liu et al., 2018; Zhou et al., 2014). Nocturnal SUHII dominated in the coastal city of Chittagong (Fig. 4), a result similar to Jauregui (1997). This nighttime feature may be associated with significant warming of the Indian Ocean and the Bay of Bengal over the last few years (Panmei, Divakar Naidu, & Mohtadi, 2017), as well as differential, evaporative cooling due to impervious surfaces (Ojeh, Balogun, & Okhimamhe, 2016), surface roughness related vertical mixing (Hu et al., 2016) and differences in other physical processes related to the release of anthropogenic heat (Wang et al., 2017).

One notable feature observed is the change in diurnal range, both at the annual and the monthly scales, over the cities. Chittagong had a strong narrowing in annual DTR, followed by Rajshahi (Fig. 4). At the monthly scale, however, the narrowing of DTR was more pronounced during the winter months (December–February) than during the monsoon, similar to that observed in data recorded at stations in Bangladesh (Abdullah et al., 2021) and with downscaled climate data (Mourshed, 2011). Maximum land temperature tends to occur in the afternoon and minimum temperature in the early dawn, so TERRA may have underestimated DTR in this work. Other MODIS sensors (such as Aqua) which acquire data during midday and early morning, may be used to corroborate the DTR variability in the study area. Urban expansion affects the minimum temperature to a greater degree than maximum temperature, and this reduction in day-night temperature variability in the dry season has been previously observed (Argüeso et al., 2014). Huang et al. (2016) noted that the amplitude of annual daytime LST is enhanced due to urbanisation in China, resulting in a narrower DTR in Beijing than in Shanghai. Hence, the impact of UHIs on annual temperature cycle (ATC) is warranted. The temporal fluctuation of SUHII can also be associated with rapid land cover changes and crop phenology (Quan et al., 2016), multiple reflection by 3-D urban structures, a reduction of evapotranspiration due to an abundance of impermeable surfaces (Wang, Berardi, & Akbari, 2016) and differential cooling rates during the early evening transition period (Hu et al., 2016). As far as land cover change is concerned, the large cities of Bangladesh have probably experienced a greater rate of change than most other cities on the globe, a rate primarily driven by high rural-urban migration (see Kant et al., 2018).

The correlation between mean day and nighttime temperature was plotted to understand whether factors affecting temperatures during the daytime were different to nighttime (Fig. 6). The analysis showed a statistically significant correlation ($R^2 = 0.50$; $p = 0.00$) across cities, suggesting that drivers influencing SUHI intensity were generally identical (Table 2). This finding contrasts with that of Peng et al. (2012) who reported no correlation between annual day and nighttime SUHII, and that drivers seemed to vary between the different global cities. Causal factors associated with the genesis of SUHII did vary in strength in this study, however population, imperviousness and lack of vegetation (greenness or live vegetation) appeared to be strong contributors to the

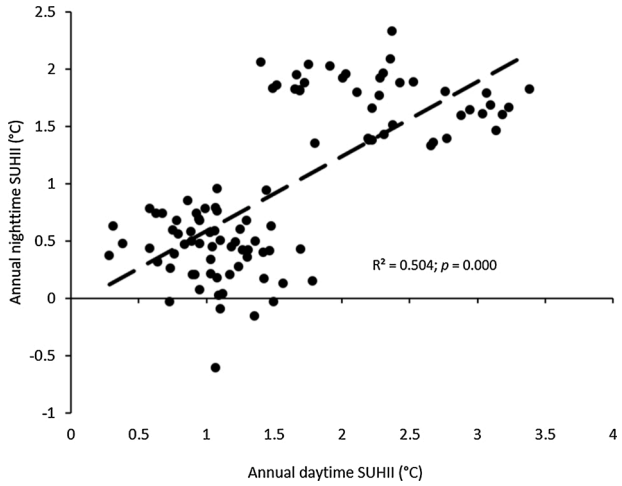

Fig. 6. Relationship between annual mean day and nighttime SUHII across cities.

rise of urban temperature.

An analysis of potential collinearity between factors indicated that NDWI, MSI and EVI were linearly dependent (Table S3), possibly due to similar moisture and/or wetness characteristics. The use of a common spectral region (i.e., near infrared) to derive these indices may also be involved. Imperviousness, represented by the biophysical composition index (BCI), was also associated with population in four of the cities, but not in Sylhet. The variables with strong linear relationships were removed from the analysis resulting in the explanatory variables having a much smaller value than the VIP threshold value of <10 (Table 1).

Human populations play a major role in shaping cities and influencing the thermal environment of urban areas, so increasing population numbers both expand city size and are accountable for the rapid transformation of natural land cover to impervious surfaces. Substituting BCI with population does not necessarily indicate that the degree of imperviousness contributes less to SUHII. Rather, the population number or density indirectly reflects the development intensity of an area and the complexity of the urban surface. For instance, a greater population means a greater number of sociocultural elements which can directly (by metabolic heating) or indirectly (by anthropogenic heat flux) affect a city's surface temperature (Rizwan, Dennis, & Chunho, 2008). In contrast, the prevalence of impermeable materials resulting from an increasing population, such as buildings, streets and other man-made features, enhance thermal admittance and high heat storage and lead to a modification in local energy balance (Mirzaei & Haghighat, 2010; Oke, 1982; Wang et al., 2016). Thus, these two factors either in combination, or singly, result in higher temperatures. Population differentials between urban and rural locations (δPOP), exhibited strong influence on the daytime SUHII for Dhaka (r = 0.92), Chittagong (r = 0.72) and Rajshahi (r = 0.50) which is in accord with studies conducted in Asian cities (Sakakibara & Matsui, 2005; Tran et al., 2006; Wu & Zhang, 2018) but contrasts with Peng et al. (2012). The negative relationship between nighttime SUHII and δPOP in the coastal cities of Chittagong and Khulna was likely to be attributed to the effect of sea breezes (Santamouris et al., 2017). The association between δBCI and temperatures during day and night was positive for Sylhet (Table 2), suggesting biophysical composition, between urban neighbourhoods, contributed positively to SUHII (Guo et al., 2015; Song & Wu, 2016; Wang et al., 2017). Despite differences in the nighttime lights between urban and rural (sub-urban) (δNTL) areas showing a positive effect on SUHII on global and regional scales (Li et al., 2020; Raj et al., 2020; Yao, Wang, Huang, Niu, Liu et al., 2018), its effect on day and nighttime temperature was negative for Dhaka (Table 2), although a strong to moderate association can be seen for the other cities, except for Khulna at night (r = −0.625). This reinforces the idea that human populations, along with enhanced socioeconomic activities, are primarily responsible for local warming, especially in Bangladesh cities and that factors controlling SUHII can vary between cities, even if they are within the same country or continent, a fact observed by other researchers (Alexander, 2021).

Vegetation, characterised by δEVI, showed a consistently negative relationship with day and nighttime SUHII, with the exception of Khulna during the night (Table 2). Previous studies have emphasised the role of greenness in moderating urban temperature, especially during daytime (Chakraborty & Lee, 2019; Chen et al., 2017; Li et al., 2020; Peng et al., 2019; Quan et al., 2016; Raj et al., 2020; Yao, Wang, Huang, Niu, Liu et al., 2018; Zhou et al., 2014). The cooling potential of an area is usually controlled by differences in evaporative cooling, variations in land use/cover, the absence of moisture and the lack of vegetation (Charabi & Bakhit, 2011; Ojeh et al., 2016; Shojaei et al., 2017). The observed relationship between δEVI and SUHII is therefore noteworthy, particularly in the context of Bangladesh cities. Green coverage (tree cover fraction) displayed inconsistent results, albeit with much lower correlations, apart from a nighttime negative relationship in Dhaka and Khulna (Table 2). This may be related to varying phenological processes (Kabano et al., 2021), an absence of shading (Giridharan & Emmanuel, 2018), seasonal variation in the LST-vegetation relationship (Qiao, Tian, & Xiao, 2013) and small signal of δVCF due to noise introduced by urban-rural differentials (Chakraborty et al., 2020). As a typical urban area in Bangladesh has a low tree density and is characterised by highly scattered vegetation patches (Rahman, Rahman, & Momotaz, 2019), any existing tree coverage may be of little help in promoting convection cooling. The cooling effect of vegetation is also dependent on its type. For instance, evergreen vegetation is substantially more effective in providing year-round benefits than deciduous vegetation (Chun & Guldmann, 2018). In contrast, a dispersed distribution of vegetation provides little cooling benefit (Quan et al., 2016), so strategically placing them in heat-exposed areas is more effective than arbitrarily aiming for a high percent of green cover in cities (Zölch, Maderspacher, Wamsler, & Pauleit, 2016). Although precise information on greenspace use (either as urban forest or parks) is sparse in Bangladesh, a previous study has shown that the existing per capita green space within a large city is very low (Jaman, Zhang, & Islam, 2020). Since areas of low LST is a typical characteristic of greenspace, these are usually the target for development during the urbanisation process (Yang, Sun, Ge, & Li, 2017), and a substantial reduction of greenspace in urban areas has been noted, intensifying the urban temperature profile (Kant et al., 2018). This practice is also seen elsewhere, with negative consequences for the local and regional thermal environment (Yang et al., 2017).

The association between albedo and SUHII was mostly negative, though daytime SUHII showed a strong positive relationship for Chittagong and Khulna (Table 2). The negative correlations may have stemmed from surface heat storage and the energy exchange capacity of urban features, as well as the lack of vegetation/greenness (Peng et al., 2012; Quan et al., 2016; Shojaei et al., 2017). While a positive relationship was expected between SUHII and δAOD (the difference of AOD between the urban and rural areas), it was found that the correlations were negative for Dhaka and Chittagong, both during the day and at night, whereas a weak relationship was observed for other cities such as Sylhet. While a similar finding was noted by Raj et al. (2020) for major Indian cities, the seasonal distribution of aerosol loading seems to have impacted on day and night SUHII in the urban areas (Pandey et al., 2014).

Annual day and nighttime positive trends in SUHII over all four cities (apart from Khulna at night) are indicative of urban area warming in Bangladesh (Table 3). This is consistent with the results of Raj et al. (2020). Although monthly SUHII trends varied, positive trends were observed during the dry months of December to February and the transitional month of November (Table 4). This highlights the impact of global warming (Giridharan & Emmanuel, 2018) and the physical processes associated with SUHI development taking place within cities

(Wang et al., 2017).

Some limitations to this study should be noted. Firstly, only remotely sensed variables were used to identify potential controlling factors of SUHII over Bangladesh cities. The inclusion of background climate (Sun, Li, Yang, & Chen, 2019), urban planning indicators (Guo, Zhou, Wu, Xiao, & Chen, 2016), landscape metrices (Peng, Hu, Dong, Liu, & Liu, 2020), black-sky albedo (Oleson et al., 2003) and waste heat information (Rizwan et al., 2008) could make future work more robust, as these variables can have a marked impact on land surface temperature. Since SUHII has strong diurnal and seasonal variations, characterising it at diurnal and seasonal scales would also be of great value. The two MODIS sensors (Aqua and Terra) record data four times a day, therefore, characterising SUHII based on the combination of the two sensors may provide a more accurate estimate of SUHII (Lai et al., 2018). Hu et al. (2016) has argued that remotely sensed LST overestimates the surface temperature of horizontal features and underestimates the surface temperature of vertical features in an urban area, so the resulting representation of the actual surface temperature may be poor. To overcome this estimation issue, the use of in-situ instrumentation is vital in providing true measurements of UHIs. Finally, the issue of reduced pixel count values (due to reduced clear sky conditions) is observed most notably in the monsoon period in Bangladesh, and hence the impact on LST and derived intensity values is most pronounced in this season. In general, the better the clear-sky conditions, the lower will be the missing pixel percentages (i.e., the greater the percentage of valid pixels). It can be assumed that the LST values recorded with 100 % valid pixels will approach the true LST climatology. Study using microwaves to remove the influence of cloud cover indicated that: i) solar radiation during the day in clear-sky situations results in higher LST values (a generally positive bias); while ii) during the night it is generally negative because of increased radiative cooling (Ermida et al., 2019). The use of in-situ instrumentation can also be used in this case to determine the validity of LST measurements.

Despite these limitations, this study provided a greater understanding of the local temperature variation within the large cities of Bangladesh and provides further information for developing possible mitigation measures.

5. Conclusion

To the best of our knowledge, this is the first study of its kind to characterise SUHII over large cities in Bangladesh, incorporating 20 years of quality-controlled, day and night, MODIS LST data, and a selection of causal factors. A buffering technique was employed to generate a rural boundary at a defined distance from the existing urban areas and SUHII was determined as the difference between these two areas. The Pearson's correlation was used to isolate those factors affecting day and night SUHII and MK tests were used to examine the temporal trends. Analysis indicated that the magnitude of annual SUHII was high for Dhaka (2.74 °C) and Chittagong (1.92 °C) during the day, however at night Chittagong had the largest magnitude (1.90 °C) followed by Dhaka (1.57 °C). Day and nighttime intensities appeared to be increasing, causing a narrowing of diurnal temperature range (DTR). Monthly analysis revealed that SUHII was greater (with few exceptions) and highly pronounced during the dry months than during wet months. An assessment of causal factors revealed that population (in terms of city size and surface cover), lack of greenness and anthropogenic forcing were the main factors affecting the temperature of Bangladesh cities. A trend assessment indicated that daytime SUHII over four out of five cities was increasing, while at night three cities were experiencing statistically insignificant positive trends, and the nighttime trend in Khulna city was decreasing. Monthly trend statistics varied significantly depending on the city, though an increasing SUHII trend in daytime was more pronounced, highlighting significant thermal variations present in city areas.

The findings of this study are expected to provide important information for further work given that global warming is likely to exacerbate urban heat island effects in the near future. This study supports progress towards the UN's sustainable development goals (SDGs) and the local climatic information detailed in this study could help in the development of area-specific mitigation measures.

Declaration of Competing Interest

The authors report no declarations of interest.

Acknowledgement

This study was supported in part by project (grant number 7188134) of the World Bank on which A. Dewan was the Principal Investigator. The funders had no role in study design, data collection and analysis, and preparation of the manuscript.

Appendix A. Supplementary data

Supplementary material related to this article can be found, in the online version, at doi:https://doi.org/10.1016/j.scs.2021.102926.

References

Abdullah, A. Y. M., Bhuian, M. H., Kiselev, G., Dewan, A., Hasan, Q. K., & Rafiuddin, M. (2021). Extreme temperature and rainfall events in Bangladesh: a comparison between coastal and inland areas. *International Journal of Climatology*. https://doi.org/10.1002/joc.6911

Alexander, C. (2021). Influence of the proportion, height and proximity of vegetation and buildings on urban land surface temperature. *International Journal of Applied Earth Observation and Geoinformation, 95*, Article 102265.

Argüeso, D., Evans, J. P., Fita, L., & Bormann, K. J. (2014). Temperature response to future urbanization and climate change. *Climate Dynamics, 42*(7-8), 2183–2199.

Bangladesh Bureau of Statistics (BBS). (2012). *Bangladesh population census 2011*. Dhaka: Ministry of Planning.

Bowler, D. E., Buyung-Ali, L., Knight, T. M., & Pullin, A. S. (2010). Urban greening to cool towns and cities: A systematic review of the empirical evidence. *Landscape and Urban Planning, 97*(3), 147–155.

Chakraborty, T., & Lee, X. (2019). A simplified urban-extent algorithm to characterize surface urban heat islands on a global scale and examine vegetation control on their spatiotemporal variability. *International Journal of Applied Earth Observation and Geoinformation, 74*, 269–280.

Chakraborty, T., Hsu, A., Manya, D., & Sheriff, G. (2020). A spatially explicit surface urban heat island database for the United States: Characterization, uncertainties, and possible applications. *ISPRS Journal of Photogrammetry and Remote Sensing, 168*, 74–88.

Chapman, S., Watson, J. E., Salazar, A., Thatcher, M., & McAlpine, C. A. (2017). The impact of urbanization and climate change on urban temperatures: A systematic review. *Landscape Ecology, 32*(10), 1921–1935.

Charabi, Y., & Bakhit, A. (2011). Assessment of the canopy urban heat island of a coastal arid tropical city: The case of Muscat, Oman. *Atmospheric Research, 101*(1-2), 215–227.

Chen, Y. C., Chiu, H. W., Su, Y. F., Wu, Y. C., & Cheng, K. S. (2017). Does urbanization increase diurnal land surface temperature variation? Evidence and implications. *Landscape and Urban Planning, 157*, 247–258.

Chun, B., & Guldmann, J. M. (2018). Impact of greening on the urban heat island: Seasonal variations and mitigation strategies. *Computers, Environment and Urban Systems, 71*, 165–176.

Connolly, C., Keil, R., & Ali, S. H. (2020). Extended urbanisation and the spatialities of infectious disease: Demographic change, infrastructure and governance. *Urban Studies, 58*(2), 245–263. https://doi.org/10.1177/0042098020910873

Corburn, J. (2009). Cities, climate change and urban heat island mitigation: Localising global environmental science. *Urban Studies, 46*(2), 413–427.

Coseo, P., & Larsen, L. (2014). How factors of land use/land cover, building configuration, and adjacent heat sources and sinks explain Urban Heat Islands in Chicago. *Landscape and Urban Planning, 125*, 117–129.

de Faria Peres, L., de Lucena, A. J., Rotunno Filho, O. C., & de Almeida França, J. R. (2018). The urban heat island in Rio de Janeiro, Brazil, in the last 30 years using remote sensing data. *International Journal of Applied Earth Observation and Geoinformation, 64*, 104–116.

Debbage, N., & Shepherd, J. M. (2015). The urban heat island effect and city contiguity. *Computers, Environment and Urban Systems, 54*, 181–194.

Deilami, K., Kamruzzaman, M., & Liu, Y. (2018). Urban heat island effect: A systematic review of spatio-temporal factors, data, methods, and mitigation measures. *International Journal of Applied Earth Observation and Geoinformation, 67*, 30–42.

Deng, C., & Wu, C. (2012). BCI: A biophysical composition index for remote sensing of urban environments. *Remote Sensing of Environment, 127*, 247–259.

Dimiceli, C., Carroll, M., Sohlberg, R., Kim, D. H., Kelly, M., & Townshend, J. R. G. (2015). *MOD44B MODIS/Terra vegetation continuous fields yearly L3 global 250 m SIN grid V006*. NASA EOSDIS Land Processes Distributed Active Archive Center.

Eckstein, D., Künzel, V., Schäfer, L., & Winges, M. (2019). *Global climate risk index 2020*. Germanwatch. Available at: https://germanwatch.org/sites/germanwatch.org/files/20-2-01e%20Global, 20.

Emmanuel, R., & Krüger, E. (2012). Urban heat island and its impact on climate change resilience in a shrinking city: The case of Glasgow, UK. *Building and Environment, 53*, 137–149.

Ermida, S. L., Trigo, I. F., DaCamara, C. C., Jiménez, C., & Prigent, C. (2019). Quantifying the clear-sky bias of satellite land surface temperature using microwave-based estimates. *Journal of Geophysical Research Atmospheres*, 844–857.

Estrada, F., Botzen, W. W., & Tol, R. S. (2017). A global economic assessment of city policies to reduce climate change impacts. *Nature Climate Change, 7*(6), 403–406.

Fu, P., & Weng, Q. (2018). Variability in annual temperature cycle in the urban areas of the United States as revealed by MODIS imagery. *ISPRS Journal of Photogrammetry and Remote Sensing, 146*, 65–73.

Gazi, M. Y., Rahman, M. Z., Uddin, M. M., & Rahman, F. A. (2020). Spatio-temporal dynamic land cover changes and their impacts on the urban thermal environment in the Chittagong metropolitan area, Bangladesh. *GeoJournal*, 1–16.

General Economics Division (GED). (2018). *Bangladesh delta plan 2100, volume 1: Strategy*. Dhaka: Bangladesh Planning Commission, Government of the People's Republic of Bangladesh. Dhaka.

Girardet, H. (2020). People and nature in an urban world. *One Earth, 2*(2), 135–137.

Giridharan, R., & Emmanuel, R. (2018). The impact of urban compactness, comfort strategies and energy consumption on tropical urban heat island intensity: A review. *Sustainable Cities and Society, 40*, 677–687.

Gong, P., Li, X., Wang, J., Bai, Y., Chen, B., Hu, T., … Zhou, Y. (2020). Annual maps of global artificial impervious area (GAIA) between 1985 and 2018. *Remote Sensing of Environment, 236*, Article 111510.

Grimm, N. B., Faeth, S. H., Golubiewski, N. E., Redman, C. L., Wu, J., Bai, X., & Briggs, J. M. (2008). Global change and the ecology of cities. *Science, 319*(5864), 756–760.

Grimmond, S. U. (2007). Urbanization and global environmental change: Local effects of urban warming. *The Geographical Journal, 173*(1), 83–88.

Guhathakurta, S., & Gober, P. (2007). The impact of the Phoenix urban heat island on residential water use. *Journal of the American Planning Association, 73*, 317–329.

Guo, G., Wu, Z., Xiao, R., Chen, Y., Liu, X., & Zhang, X. (2015). Impacts of urban biophysical composition on land surface temperature in urban heat island clusters. *Landscape and Urban Planning, 135*, 1–10.

Guo, G., Zhou, X., Wu, Z., Xiao, R., & Chen, Y. (2016). Characterizing the impact of urban morphology heterogeneity on land surface temperature in Guangzhou, China. *Environmental Modelling & Software, 84*, 427–439.

Hartz, D. A., Prashad, L., Hedquist, B. C., Golden, J., & Brazel, A. J. (2006). Linking satellite images and hand-held infrared thermography to observed neighborhood climate conditions. *Remote Sensing of Environment, 104*(2), 190–200.

Heisler, G. M., & Brazel, A. J. (2010). The urban physical environment: Temperature and urban heat islands. *Urban ecosystem ecology, 55*, 29–56.

Hodrick, R. J., & Prescott, E. C. (1997). Postwar US business cycles: An empirical investigation. *Journal of Money, Credit, and Banking*, 1–16.

Howard, L. (1833). *The climate of London: Deduced from meteorological observations* (Vol. 1). Cambridge University Press.

Hu, X. M., Xue, M., Klein, P. M., Illston, B. G., & Chen, S. (2016). Analysis of urban effects in Oklahoma City using a dense surface observing network. *Journal of Applied Meteorology and Climatology, 55*(3), 723–741.

Huang, F., Zhan, W., Voogt, J., Hu, L., Wang, Z., Quan, J., … Guo, Z. (2016). Temporal upscaling of surface urban heat island by incorporating an annual temperature cycle model: A tale of two cities. *Remote Sensing of Environment, 186*, 1–12.

Huang, X., Huang, J., Wen, D., & Li, J. (2021). An updated MODIS global urban extent product (MGUP) from 2001 to 2018 based on an automated mapping approach. *International Journal of Applied Earth Observation and Geoinformation, 95*, Article 102255.

Huq, S. (2001). Climate change and Bangladesh. *Science, 294*(5547), 1617–1618.

Im, E. S., Pal, J. S., & Eltahir, E. A. (2017). Deadly heat waves projected in the densely populated agricultural regions of South Asia. *Science Advances, 3*(8), Article e1603322.

Imhoff, M. L., Zhang, P., Wolfe, R. E., & Bounoua, L. (2010). Remote sensing of the urban heat island effect across biomes in the continental USA. *Remote Sensing of Environment, 114*(3), 504–513.

Itzhak-Ben-Shalom, H., Alpert, P., Potchter, O., & Samuel, R. (2017). MODIS summer SUHI cross-sections anomalies over the megacities of the monsoon Asia region and global trends. *The Open Atmospheric Science Journal, 11*, 121–136.

Jaman, S., Zhang, X., & Islam, F. (2020). Carbon storage and tree diversity in the urban vegetation of Dhaka city, Bangladesh: A study based on intensive field investigation. *Arboricultural Journal*, 1–17.

Jauregui, E. (1997). Heat island development in Mexico city. *Atmospheric Environment, 31*(22), 3821–3831.

Kabano, P., Lindley, S., & Harris, A. (2021). Evidence of urban heat island impacts on the vegetation growing season length in a tropical city. *Landscape and Urban Planning, 206*, Article 103989.

Kafy, A. A., Rahman, M. S., Hasan, M. M., & Islam, M. (2020). Modelling future land use land cover changes and their impacts on land surface temperatures in Rajshahi, Bangladesh. *Remote Sensing Applications Society and Environment, 18*, Article 100314.

Kalnay, E., & Cai, M. (2003). Impact of urbanization and land-use change on climate. *Nature, 423*(6939), 528–531.

Kant, Y., Azim, S., & Mitra, D. (2018). Analyzing the influence of urban growth on thermal environment through demographic, environmental, and physical parameters in Bangladesh. *Land-atmospheric research applications in south and Southeast Asia* (pp. 613–639). Cham: Springer.

Kendall, M. G. (1948). *Rank correlation methods*. Michigan: C. Griffin.

Kerr, Y. H., Lagouarde, J. P., Nerry, F., & Ottlé, C. (2004). Land surface temperature retrieval techniques and applications: Case of the AVHRR. *Thermal remote sensing in land surface processing* (pp. 55–131). CRC Press.

Kotharkar, R., Ramesh, A., & Bagade, A. (2018). Urban heat island studies in South Asia: A critical review. *Urban Climate, 24*, 1011–1026.

Krayenhoff, E. S., Moustaoui, M., Broadbent, A. M., Gupta, V., & Georgescu, M. (2018). Diurnal interaction between urban expansion, climate change and adaptation in US cities. *Nature Climate Change, 8*(12), 1097–1103.

Lai, J., Zhan, W., Huang, F., Quan, J., Hu, L., Gao, L., & Ju, W. (2018). Does quality control matter? Surface urban heat island intensity variations estimated by satellite-derived land surface temperature products. *ISPRS Journal of Photogrammetry and Remote Sensing, 139*, 212–227.

Landsberg, H. E. (1981). *The urban climate*. New York: Academic press.

Lazzarini, M., Marpu, P. R., & Ghedira, H. (2013). Temperature-land cover interactions: The inversion of urban heat island phenomenon in desert city areas. *Remote Sensing of Environment, 130*, 136–152.

Li, D., Liao, W., Rigden, A. J., Liu, X., Wang, D., Malyshev, S., & Shevliakova, E. (2019). Urban heat island: Aerodynamics or imperviousness? *Science Advances, 5*, eaau4299.

Li, J., Song, C., Cao, L., Zhu, F., Meng, X., & Wu, J. (2011). Impacts of landscape structure on surface urban heat islands: A case study of Shanghai, China. *Remote Sensing of Environment, 115*, 3249–3263.

Li, L., Zha, Y., & Zhang, J. (2020). Spatially non-stationary effect of underlying driving factors on surface urban heat islands in global major cities. *International Journal of Applied Earth Observation and Geoinformation, 90*, Article 102131.

Liao, W., Liu, X., Li, D., Luo, M., Wang, D., Wang, S., … Hubacek, K. (2018). Stronger contributions of urbanization to heat wave trends in wet climates. *Geophysical Research Letters, 45*(20), 11–310.

Lin, F. J. (2008). Solving multicollinearity in the process of fitting regression model using the nested estimate procedure. *Quality & Quantity, 42*(3), 417–426.

Liu, H. Q., & Huete, A. R. (1995). A feedback-based modification of the NDVI to minimize canopy background and atmospheric noise. *IEEE Transactions on Geoscience and Remote Sensing, 33*, 457–465.

Liu, Z., He, C., Zhang, Q., Huang, Q., & Yang, Y. (2012). Extracting the dynamics of urban expansion in China using DMSP-OLS nighttime light data from 1992 to 2008. *Landscape and Urban Planning, 106*(1), 62–72.

Ma, J., Guo, J., Ahmad, S., Li, Z., & Hong, J. (2020). Constructing a new inter-calibration method for DMSP-OLS and NPP-VIIRS nighttime light. *Remote Sensing, 12*(6), 937.

Malings, C., Pozzi, M., Klima, K., Bergés, M., Bou-Zeid, E., & Ramamurthy, P. (2017). Surface heat assessment for developed environments: Probabilistic urban temperature modeling. *Computers, Environment and Urban Systems, 66*, 53–64.

Mann, H. B. (1945). Nonparametric tests against trend. *Econometrica: Journal of the Econometric Society*, 245–259.

Manoli, G., Fatichi, S., Schläpfer, M., Yu, K., Crowther, T. W., Meili, N., … Bou-Zeid, E. (2019). Magnitude of urban heat islands largely explained by climate and population. *Nature, 573*(7772), 55–60.

Mathew, A., Khandelwal, S., & Kaul, N. (2017). Investigating spatial and seasonal variations of urban heat island effect over Jaipur city and its relationship with vegetation, urbanization and elevation parameters. *Sustainable Cities and Society, 35*, 157–177.

Mathew, A., Khandelwal, S., Kaul, N., & Chauhan, S. (2018). Analyzing the diurnal variations of land surface temperatures for surface urban heat island studies: Is time of observation of remote sensing data important? *Sustainable Cities and Society, 40*, 194–213.

McFeeters, S. K. (1996). The use of the Normalized Difference Water Index (NDWI) in the delineation of open water features. *International Journal of Remote Sensing, 17*(7), 1425–1432.

Mirzaei, P. A., & Haghighat, F. (2010). Approaches to study urban heat island–abilities and limitations. *Building and Environment, 45*(10), 2192–2201.

Mora, C., Dousset, B., Caldwell, I. R., Powell, F. E., Geronimo, R. C., Bielecki, C. R., … Lucas, M. P. (2017). Global risk of deadly heat. *Nature Climate Change, 7*(7), 501–506.

Moretti, E. (2014). *Cities and growth*. The UK: International Growth Center.

Mourshed, M. (2011). The impact of the projected changes in temperature on heating and cooling requirements in buildings in Dhaka, Bangladesh. *Applied Energy, 88*(11), 3737–3746.

Ojeh, V. N., Balogun, A. A., & Okhimamhe, A. A. (2016). Urban-rural temperature differences in Lagos. *Climate, 4*(2), 29.

Oke, T. R. (1982). The energetic basis of the urban heat island. *Quarterly Journal of the Royal Meteorological Society, 108*(455), 1–24.

Oleson, K. W., Bonan, G. B., Schaaf, C., Gao, F., Jin, Y., & Strahler, A. (2003). Assessment of global climate model land surface albedo using MODIS data. *Geophysical Research Letters, 30*(8).

Pandey, A. K., Singh, S., Berwal, S., Kumar, D., Pandey, P., Prakash, A., … Kumar, K. (2014). Spatio–temporal variations of urban heat island over Delhi. *Urban Climate, 10*, 119–133.

Panmei, C., Divakar Naidu, P., & Mohtadi, M. (2017). Bay of Bengal exhibits warming trend during the Younger Dryas: Implications of AMOC. *Geochemistry Geophysics Geosystems, 18*(12), 4317–4325.

Parsaee, M., Joybari, M. M., Mirzaei, P. A., & Haghighat, F. (2019). Urban heat island, urban climate maps and urban development policies and action plans. *Environmental Technology & Innovation, 14*, Article 100341.

Peng, J., Hu, Y., Dong, J., Liu, Q., & Liu, Y. (2020). Quantifying spatial morphology and connectivity of urban heat islands in a megacity: A radius approach. *The Science of the Total Environment, 714*, Article 136792.
Peng, S., Feng, Z., Liao, H., Huang, B., Peng, S., & Zhou, T. (2019). Spatial-temporal pattern of, and driving forces for, urban heat island in China. *Ecological Indicators, 96*, 127–132.
Peng, S., Piao, S., Ciais, P., Friedlingstein, P., Ottle, C., Bréon, F. M., … Myneni, R. B. (2012). Surface urban heat island across 419 global big cities. *Environmental Science & Technology, 46*(2), 696–703.
Pyrgou, A., Hadjinicolaou, P., & Santamouris, M. (2020). Urban-rural moisture contrast: Regulator of the urban heat island and heatwaves' synergy over a mediterranean city. *Environmental Research, 182*, Article 109102.
Qiao, Z., Tian, G., & Xiao, L. (2013). Diurnal and seasonal impacts of urbanization on the urban thermal environment: a case study of Beijing using MODIS data. *ISPRS Journal of Photogrammetry and Remote Sensing, 85*, 93–101.
Quan, J., Zhan, W., Chen, Y., Wang, M., & Wang, J. (2016). Time series decomposition of remotely sensed land surface temperature and investigation of trends and seasonal variations in surface urban heat islands. *Journal of Geophysical Research Atmospheres, 121*(6), 2638–2657.
Rahman, M. M., Rahman, M. M., & Momotaz, M. (2019). Environmental quality evaluation in Dhaka City Corporation–using satellite imagery. *Proceedings of the Institution of Civil Engineers-Urban Design and Planning, 172*(1), 13–25.
Rahman, M., Avtar, R., Yunus, A. P., Dou, J., Misra, P., Takeuchi, W., … Kharrazi, A. (2020). Monitoring effect of spatial growth on land surface temperature in Dhaka. *Remote Sensing, 12*(7), 1191.
Rai, R., Zhang, Y., Paudel, B., Li, S., & Khanal, N. R. (2017). A synthesis of studies on land use and land cover dynamics during 1930–2015 in Bangladesh. *Sustainability, 9*(10), 1866.
Raj, S., Paul, S. K., Chakraborty, A., & Kuttippurath, J. (2020). Anthropogenic forcing exacerbating the urban heat islands in India. *Journal of Environmental Management, 257*, Article 110006.
Ren, C., Ng, E. Y. Y., & Katzschner, L. (2011). Urban climatic map studies: A review. *International Journal of Climatology, 31*, 2213–2233.
Ren, G. Y., Chu, Z. Y., Chen, Z. H., & Ren, Y. Y. (2007). Implications of temporal change in urban heat island intensity observed at Beijing and Wuhan stations. *Geophysical Research Letters, 34*(5).
Rizwan, A. M., Dennis, L. Y., & Chunho, L. I. U. (2008). A review on the generation, determination and mitigation of Urban Heat Island. *Journal of the Environmental Sciences, 20*, 120–128.
Rock, B. N., Vogelmann, J. E., Williams, D. L., Vogelmann, A. F., & Hoshizaki, T. (1986). Remote Detection of Forest Damage: Plant responses to stress may have spectral "signatures" that could be used to map, monitor, and measure forest damage. *Bioscience, 36*(7), 439–445.
Rodríguez, L. R., Ramos, J. S., de la Flor, F. J. S., & Domínguez, S.Á. (2020). Analyzing the Urban Heat Island: Comprehensive methodology for data gathering and optimal design of mobile transects. *Sustainable Cities and Society, 55*, Article 102027.
Roth, M. (2007). Review of urban climate research in (sub) tropical regions. *International Journal of Climatology: A Journal of the Royal Meteorological Society, 27*(14), 1859–1873.
Roy, S., Pandit, S., Eva, E. A., Bagmar, M. S. H., Papia, M., Banik, L., … Razi, M. A. (2020). Examining the nexus between land surface temperature and urban growth in Chattogram Metropolitan Area of Bangladesh using long term Landsat series data. *Urban Climate, 32*, Article 100593.
Sakakibara, Y., & Matsui, E. (2005). Relation between heat island intensity and city size indices/urban canopy characteristics in settlements of Nagano basin, Japan. *Geographical Review of Japan, 78*(12), 812–824.
Salata, F., Golasi, I., Petitti, D., de Lieto Vollaro, E., Coppi, M., & de Lieto Vollaro, A. (2017). Relating microclimate, human thermal comfort and health during heat waves: An analysis of heat island mitigation strategies through a case study in an urban outdoor environment. *Sustainable Cities and Society, 30*, 79–96.
Santamouris, M., Haddad, S., Fiorito, F., Osmond, P., Ding, L., Prasad, D., … Wang, R. (2017). Urban heat island and overheating characteristics in Sydney, Australia. An analysis of multiyear measurements. *Sustainability, 9*(5), 712.
Schwarz, N., Lautenbach, S., & Seppelt, R. (2011). Exploring indicators for quantifying surface urban heat islands of European cities with MODIS land surface temperatures. *Remote Sensing of Environment, 115*(12), 3175–3186.
Sen, P. K. (1968). Estimates of the regression coefficient based on Kendall's tau. *Journal of the American Statistical Association, 63*(324), 1379–1389.
Seto, K. C., Fragkias, M., Güneralp, B., & Reilly, M. K. (2011). A meta-analysis of global urban land expansion. *PloS One, 6*(8), Article e23777.
Shojaei, P., Gheysari, M., Myers, B., Eslamian, S., Shafieiyoun, E., & Esmaeili, H. (2017). Effect of different land cover/use types on canopy layer air temperature in an urban area with a dry climate. *Building and Environment, 125*, 451–463.
Song, Y., & Wu, C. (2016). Examining the impact of urban biophysical composition and neighboring environment on surface urban heat island effect. *Advances in Space Research, 57*, 96–109.
Sulla-Menashe, D., & Friedl, M. A. (2018). *User guide to collection 6 MODIS land cover (MCD12Q1 and MCD12C1) product*. available at https://lpdaac.usgs.gov/documents/101/MCD12_User_Guide_V6.pdf.
Sun, R., Li, Y., Yang, X., & Chen, L. (2019). Understanding the variability of urban heat islands from local background climate and urbanization. *Journal of Cleaner Production, 208*, 743–752.
Tan, X., Sun, X., Huang, C., Yuan, Y., & Hou, D. (2021). Comparison of cooling effect between green space and water body. *Sustainable Cities and Society*, Article 102711.
Tomlinson, C. J., Chapman, L., Thornes, J. E., & Baker, C. J. (2012). Derivation of Birmingham's summer surface urban heat island from MODIS satellite images. *International Journal of Climatology, 32*(2), 214–224.
Tran, H., Uchihama, D., Ochi, S., & Yasuoka, Y. (2006). Assessment with satellite data of the urban heat island effects in Asian mega cities. *International Journal of Applied Earth Observation and Geoinformation, 8*(1), 34–48.
Trotter, L., Dewan, A., & Robinson, T. (2017). Effects of rapid urbanisation on the urban thermal environment between 1990 and 2011 in Dhaka Megacity, Bangladesh. *AIMS Environmental Science, 4*(1), 145–167.
Wan, Z. (2014). New refinements and validation of the collection-6 MODIS land-surface temperature/emissivity product. *Remote Sensing of Environment, 140*, 36–45.
Wang, K., Jiang, S., Wang, J., Zhou, C., Wang, X., & Lee, X. (2017). Comparing the diurnal and seasonal variabilities of atmospheric and surface urban heat islands based on the Beijing urban meteorological network. *Journal of Geophysical Research Atmospheres, 122*(4), 2131–2154.
Wang, K., Wang, J., Wang, P., Sparrow, M., Yang, J., & Chen, H. (2007). Influences of urbanization on surface characteristics as derived from the Moderate-Resolution Imaging Spectroradiometer: A case study for the Beijing metropolitan area. *Journal of Geophysical Research Atmospheres, 112*(D22).
Wang, Y., Berardi, U., & Akbari, H. (2016). Comparing the effects of urban heat island mitigation strategies for Toronto, Canada. *Energy and Buildings, 114*, 2–19.
Wu, H., Ye, L. P., Shi, W. Z., & Clarke, K. C. (2014). Assessing the effects of land use spatial structure on urban heat islands using HJ-1B remote sensing imagery in Wuhan, China. *International Journal of Applied Earth Observation and Geoinformation, 32*, 67–78.
Wu, L., & Zhang, J. (2018). Assessing population movement impacts on urban heat island of Beijing during the Chinese New Year holiday: Effects of meteorological conditions. *Theoretical and Applied Climatology, 131*(3–4), 1203–1210.
Wu, J., He, S., Peng, J., Li, W., & Zhong, X. (2013). Intercalibration of DMSP-OLS night-time light data by the invariant region method. *International Journal of Remote Sensing, 34*(20), 7356–7368.
Wu, A., Xiong, X., Doelling, D. R., Morstad, D., Angal, A., & Bhatt, R. (2013). Characterization of terra and aqua MODIS VIS, NIR, and SWIR spectral bands' calibration stability. *IEEE Transactions on Geoscience and Remote Sensing, 51*, 4330–4338.
Yang, J., Sun, J., Ge, Q., & Li, X. (2017). Assessing the impacts of urbanization-associated green space on urban land surface temperature: A case study of Dalian, China. *Urban Forestry & Urban Greening, 22*, 1–10.
Yang, Y., Zheng, Z., Yim, S. Y., Roth, M., Ren, G., Gao, Z., … Li, Y. (2020). PM2. 5 pollution modulates wintertime urban heat island intensity in the Beijing-Tianjin-Hebei Megalopolis, China. *Geophysical Research Letters, 47*(1). e2019GL084288.
Yao, R., Wang, L., Huang, X., Niu, Y., Chen, Y., & Niu, Z. (2018). The influence of different data and method on estimating the surface urban heat island intensity. *Ecological Indicators, 89*, 45–55.
Yao, R., Wang, L., Huang, X., Niu, Z., Liu, F., & Wang, Q. (2018). Temporal trends of surface urban heat islands and associated determinants in major Chinese cities. *The Science of the Total Environment, 609*, 742–754.
Zhou, D., Zhao, S., Liu, S., Zhang, L., & Zhu, C. (2014). Surface urban heat island in China's 32 major cities: Spatial patterns and drivers. *Remote Sensing of Environment, 152*, 51–61.
Zhou, L., Dickinson, R. E., Tian, Y., Fang, J., Li, Q., Kaufmann, R. K., … Myneni, R. B. (2004). Evidence for a significant urbanization effect on climate in China. *Proceedings of the National Academy of Sciences United States of America, 101*(26), 9540–9544.
Zölch, T., Maderspacher, J., Wamsler, C., & Pauleit, S. (2016). Using green infrastructure for urban climate-proofing: An evaluation of heat mitigation measures at the micro-scale. *Urban Forestry & Urban Greening, 20*, 305–316.